Advances in Science and Technology Research Journal

Advances in Science and Technology Research Journal, 2026, 20(9), 411–423
https://doi.org/10.12913/22998624/224855
ISSN 2299-8624, License CC-BY 4.0

Received: 2026.05.19
Accepted: 2026.07.01
Published: 2026.08.01

Assessment of thermal behavior for phase transition material through dynamic heating-cooling scenario energy system

Dwi Chandra Adhitya[1], Dwi Rahmalina[1*], Ismail[1], Abid Fahreza Alphanoda[1], Reza Abdu Rahman[1]

[1] Department of Mechanical Engineering, Faculty of Engineering, Universitas Pancasila, Srengseng Sawah, Jagakarsa, DKI Jakarta 12640, Indonesia
* Corresponding author's e-mail: drahmalina@univpancasila.ac.id

ABSTRACT

Technology energy storage rapidly growth as it plays essential position for the energy transition in modern era, particularly for thermal energy storage (TES). It expands largely considering its flexibility and scalability for different load and application in thermal system. The usage of phase change material (PCM) for TES provides technical benefit since it widely available and cost effective. However, specific working indicator for the materials are varied notably, making the development for the PCM and its intended application become complex to assure process control of the energy transfer for each configuration. The present work offers working assessment for six type PCM which divided into low-temperature (LT) and high-temperature (HT) groups. The assessment was performed experimentally on the heating cycle at different rate, followed with different loading scenario for discharge the energy. The initial indicator comes from different melting behavior for each PCM, varying between 61–64.8 °C with ΔH 148.2–178.5 J/g for LT-group, and 92.4–119.4 °C with ΔH 174.3–275.6 J/g. The challenge starts with cooling function (freezing) as each material experience deviation on transition for phase temperature between 4.8–6.5 °C for LT-group with the highest deviation is obtained from HT-group. The maximum heating rate for LT-group varies between 2.18–5.66 °C/min while HT-group indicates a lower maximum heating rate between 1.7–3.33 °C/min. Dynamic cooling causes significant variation for the LT-group, specifically between slow and rapid cooling with maximum variation of 1.4 °C/min, indicating the PCM for this group sensitive to different discharge mechanism. In contrast, HT-group demonstrate unsubstantial change for the cooling rate which remain below 1 °C/min for all designed discharge operation.

Keywords: energy, enthalpy, fatty acids, polyols, wax.

INTRODUCTION

Demand energy global raises annually along with technology advancement, high standard modern civilization and global trading. Dependence on conventional source like fossil fuel brings the challenge of potential crisis as the source has limited capacity [1] and challenge of global warming from fossil fuel combustion [2]. It pushes society to transform using cleaner technology like renewable wind power [3–5] which has proven commercially. Different source also possible to be utilized, making researcher assess the potential of waste as reliable energy source [6] and solar power. All possible options are further optimized, hoping it transform entirely the conventional source into renewable and sustainable cleaner energy.

Transforming energy technology using renewable source highly linked with storage mechanism for the produced system. This also important to utilize bio-based material to develop cleaner energy technologies and material for energy system [7]. The aspect is successfully in thermal system since it supported by thermal energy storage (TES) as storage component for the infrastructure. TES unit rapidly growth, specifically the system which utilizes phase change material (PCM). The

operational with PCM offers the system to reach higher storage capability, including the possibility to choose suitable material that commercially available. The classification is made for a clearer purpose, typically depends on the temperature requirement of heating application [8]. It divides the PCM into two distinct categories: the low temperature (LT, 50–70 °C) and high temperature (HT, > 90 °C) PCM [9–11]. Despite some advantageous properties of the material, challenge still appears for each category which make deeper analysis and continuous evaluation are conducted to enhance the reliability of the TES unit.

Paraffin wax (HYW) is one of common material for TES which included in the category of LT-PCM. Improving the HYW generally conducted by focusing on phase behavior modification and conductivity (λ_{TC}) improvement. The work [12] offered innovative method by utilizing activated carbon with pore volume 0.138 cc/g, achieving the λ_{TC} for the composite to ~5 mW/m·K. The solution indicated the optimal capacity based on ΔH about 0.187 kJ/g. Theriselvam et al. [13] developed coating HYW with epoxy and mixed with biochar to prevent leakage. The produced composite achieved the lowest leakage rate after using 0.35/0.45 biochar with hardness (Shore-D) more than 60, allowing for excellence physical strength of the produced PCM. Alturki et al. [14] used HYW as PCM for metallic solar receiver. The system's efficiency improved after using HYW according to thermal efficiency enhancement about 16.6% which followed by exergy efficiency around 44%. The studies signify the positive achievement when introducing HYW as PCM for the given thermal system.

Different LT-group as PCM for TES unit are also available in market grade like stearic (FA-1 STE) and palmitic (FA-2 PAL). The development of the two materials is taken according to the intended application. For example, development of nano doping using nanotubes-Al_2O_3 for FA-1 STE improved the λ_{TC} with enhancement about 132.7% and maintain the ΔH above 200 J/g [15]. The study [16] conducted assessment for the potential application of FA-1 STE as bio PCM for the operation on building wall, highlighting the major role of chemical chain which altered the mechanism of heat absorption along with phase change. Dubey et al. [17] evaluated FA-1 STE as PCM for solar still unit, showing the positive improvement when using the PCM which increased the 4E aspects of the developed system. The type FA-2 PAL is possible for direct operation, obtaining the photothermal conversion which enhanced when using g-C_3N_4 for improving the optical properties with bandgap 2.7 eV [18]. Polyurethane is used as the matrix for FA-2 PAL based on the function related with direct conversion, giving an excellent capability as leakage free composite with ΔH 184.8 J/g that also enhanced using TiO_2 [19]. New attention is intended to consider the recyclability for FA-2 PAL through bio material with remarkable ΔH > 150 J/g [20]. Various modifications clearly represent the development of the component to achieve ideal operational consideration as PCM.

The PCM comes from HT-group offers wider possible application. It is based the unique properties of HT group PCM like xylitol (XYT), sorbitol (SRB) and erythritol (ERT), particularly for the energy density based on higher ΔH and solid-liquid transition temperature above 90 °C which makes the capability to be applied as thermal battery [21]. Moreover, the feasibility of the HT group is supported by reliable source and sustainability, including the recyclability option related to bio PCM [22]. Focusing the application as TES unit, SRB is designed in tank-based storage configuration supported by wire mesh which achieves thermal performance exceed 40% as the result of excellent heat distribution [23]. XYT was developed as binary system PCM with urea and organic acids, producing flexible temperature transition between 70–90 °C with ΔH more than 210 J/g [24]. Navarro et al. analysed in detail regarding the crystallization capability of XYT, showing aspect seed size (300–700 μm) and shear rate offer functional control latent heat release at specific operating temperature of the designed TES unit [25]. Chenxu et al. evaluated triggering-based XYT using nitrogen (N_2) as prevention of subcooling condition on the operation of TES unit [26].

HT-group based on ERT generally developed on the higher function considering its suitable reversibility. Hou et al. combined the recrystallized ability of ERY with XYT for TES unit supported by helical coil (double), showing the system capacity reached 10 MJ with power indicator (cooling) at the rate 0.31 kW [27]. Fang et al. modified structure of ERT with PVP to form dynamic bond of C═O with key attention to enhance the supercooling capacity of ERT and crystallization trigger at low temperature [28]. The modifications bring technical benefit to store the material at 0 °C for three months without

indicating any exothermic release, allowing for a controllable heat release from the TES unit for specific application. For broader application, the ERT is applicable for operational as mobilized TES [29]. It shows the key flexibility for using TES unit which developed based on the suitable PCM candidate and properties.

The development of the two group LT and HT PCM reveal the general challenge for each material, specifically the λ_{TC} and thermal response. At the operational level, real challenge becomes more complex due to dynamic energy transfer (charging/discharging) between the material/system which greatly affect the overall performance of the TES unit as well as the system [30]. For the operational charging, Yuan et al. [31] assessed the operation condition of unit TES for rural heating, clearly indicating the effect of thermal response due to material arrangement, thickness and heating duration require further combination for the design and operation protocol. The study [32] evaluated the heating rate variation for TES unit, implying the identic phenomenon that system design and operation characteristic must be adjusted to ensure effective working performance of the system. It also important to understand the impact at material level and modification of thermal properties [33], including the effect of heating/cooling rate. Jiang et al. [34] studied numerically for the charge level related to the PCM and concluded the role of sensible heating becomes more dominant at the early-final stage of operation. Besides, certain system demand for rapid discharge of the PCM to provide rapid energy transfer for sensitive components and application [35].

The reviewed previous studies demonstrate the potential application of commercial PCM and crucial role on the modification of each material based on the designed case. However, the basic consideration at the operational level by combining the assessment on thermal behavior under dynamic condition during charge (heating) and discharge (cooling) less discussed as practical knowledge to understand each type of PCM from each group. It becomes important to address the issues experimentally as it related with operational level that meet the criteria to various TES configuration while keep the specific working indicator identic during energy transfer. To address the gap, it is required to fully evaluate the operation of various PCM using different rating operation activity, including the function of heating/cooling. It is essential to address the basic evaluation and determine the key characteristic of TES unit for the proposed material. The current work is designed to deliver working performance to adjust the operation determination based on the key characteristic of PCM, providing essential knowledge to further progressing the applicable TES unit for different thermal system.

MATERIALS AND METHOD

This work is designed to assess the potential of TES using PCM which come from low-temperature (LT) and high-temperature (HT) group. The PCM for LT-group includes wax (HYW), stearic (FA-1 STE) and palmitic (FA-2 PAL) while HT-group consists xylitol (SA-1 XYT), sorbitol (SA-2 SRB) and erythritol (SA-3 ERT). Each material is considered as feasible candidate for the development in thermal application based on their melting point. The materials were obtained from local supplier as commercial grade material (purity above 95%) and directly processed as received (a.r.) without additional modification. To obtain the physical characteristic and thermal properties of the PCMs, several characterizations were performed. Fourier-Transform Infrared (FTIR, Perkin Elmer) was taken to obtain the chemical structure for each PCM, continue with X-Ray diffraction (XRD, PANalytical) to obtain the phase characteristic. Then, differential scanning calorimetry (DSC, NETZSCH) was taken to obtain the phase change characteristic. For this characterization, 16.5 mg of each PCM was placed in the crucible (Al_2O_3), heating at rate 10 K/min from 30 to 150 °C and holding at 150 °C for 10 seconds before cooling down to 30 °C with the same rate using nitrogen as cooling medium and gas atmosphere. Then, thermogravimetric (TGA, NETZSCH) was taken to observe the limit working temperature for each PCM at heating rate 10 K/min.

The actual operational TES allows for variation of heating intake through charge cycle with various load characteristic during discharge. Therefore, the assessment scenario was taken to accommodate the dynamic heating-cooling which represent the actual operation of TES unit. Recent trend indicates direct charge TES with electric heater owing to excellent control operation and possibility to store clean electricity [39–41]. In case of direct heating, dynamic heating scenario was obtained by varying the power input to the

heater, allowing for observing the temperature evolution and charge pattern for each PCM. For discharge cycle, it can conducted under various mechanism like using ambient air-free convection [42], flowing air-forced convection [43] and liquid [44]. Thus, the dynamic cooling assessment was designed to meet the criteria to observe the characteristic of heat releasement under different load for each PCM.

The temperature-energy response was further used as an operational indicator to evaluate the behavior of the PCMs during charging and discharging. This approach is consistent with previous heat storage evaluation using a hybrid energy-temperature method, which was developed to estimate the thermal capacity of solid-liquid phase change materials in heat storage systems [45]. In addition, previous work on active latent heat storage showed that the rate performance of PCM systems is strongly influenced by material stabilization and repeated charge-discharge behavior [46]. Therefore, the present experimental design links material characterization with dynamic operational response, allowing LT- and HT-PCMs to be compared under consistent heating-cooling scenarios.

Figure 1a shows the representation of experimental process which performed in this study. The system equipped with heating control circuit and temperature monitor. In this study, the operation activity is defined based on heating (thermal charging/TC) and cooling (thermal discharge/TD) stage. Each function is divided into slow operation (STC/STD), medium (MTC/MTD) and rapid (RTC/RTD). In term of heating intake, the level is set from the input power for the heater: 0.1 kW (STC), 0.15 kW (MTC) and 0.2 kW (RTC). The lower heating point was 40 °C for all PCM while the upper temperature limit was 100 °C (LT-group), 120 °C (SA-1 and SA-2 from HT-group), and 140 °C for SA-3 due to the melting range of the material around 120 °C. For the cooling operation, passive air mechanism is taken as STD, while MTD using force air circulation and

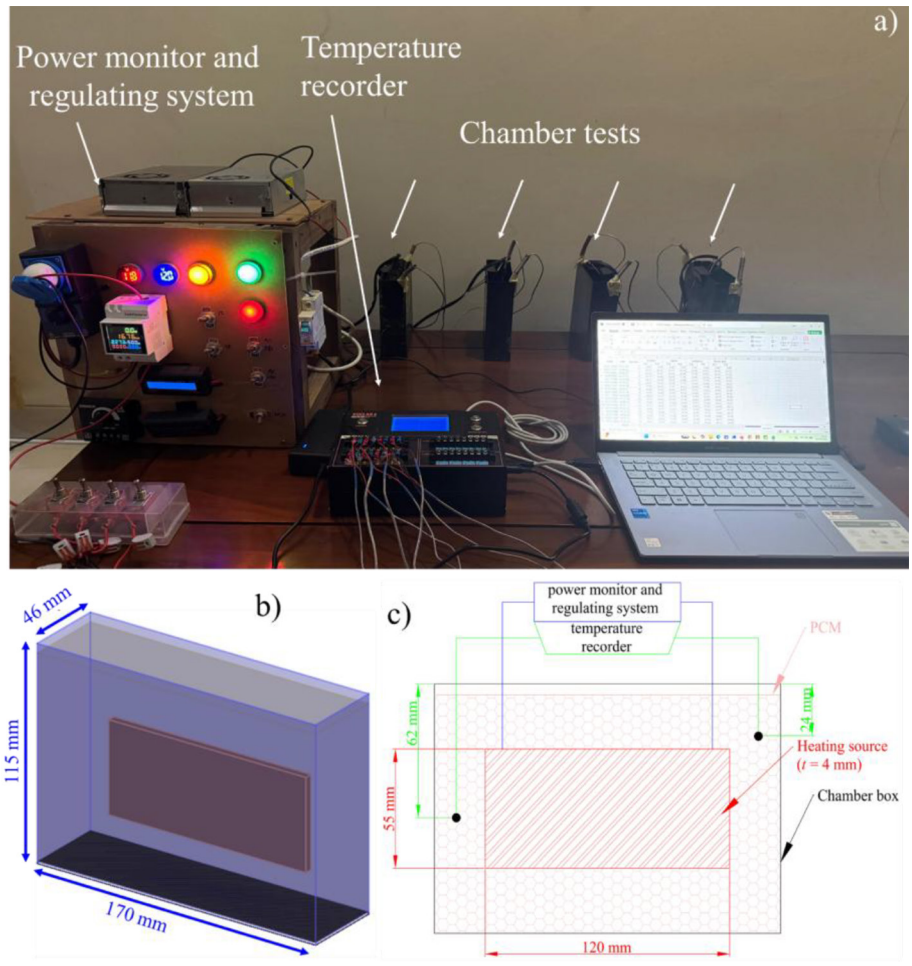

Figure 1. Apparatus for dynamic-cooling assessment scenario (a), the chamber test (b), schematic and dimension of the components (c)

RTD was done by storing the chamber inside cold liquid. Thus, the designed operation activity has represented the dynamic heating-cooling which suitable according general TES system.

The experimental procedure was started by pouring the molten PCM (0.85 kg) to the chamber test (Figure 1b). Then, sample was left to cool down at room temperature. Then, sample processed to the designed dynamic heating per design scenario. The heating power was regulated by the controller and monitored real time using the electric meter. Temperature of the PCM was recorded at two different positions (Figure 1c) using K-type thermocouple with absolute error 0.8%. After reaching the maximum charge point, sample was processed to discharge test according to the designed case. Each test was carried independently for each PCM and repeated three times. The average measurement for each test was taken as the median value and used for plotting the data and analysis to determine the specific heating/cooling rate.

RESULTS AND DISCUSSION

The FTIR assessment is taken to evaluate the chemical structure of the tested PCM. The obtained spectrum is plotted in Figure 2a, giving a clear indication for the variation of constituent element for each PCM. For example, HYW consist of saturated C−H bonding with a simple profile of stretching C−H at 2900 cm^{-1}. The peak for the area also appears for FA-1 and FA-2 with relatively weaker peak than HYW while all HT-group indicates the weakest peak among all PCM. Specific identity for HT-group is observed as the function of O−H with broad peak around 3300 cm^{-1}, followed with multiple C−O stretching at the 1050 cm^{-1}. Specifically for FA group, definitive identity appears as the carbonyl profile at 1700 cm^{-1} [47]. The XRD pattern for LT-group demonstrates clear identity of sharp peaks at two relatively similar 2θ, demonstrating good crystallinity for the materials (Figure 2b). Each PCM in HT-group demonstrates different 2θ. The multi-peaks appearance for SA-2 reveals the amorphous phase while SA-1 indicates excellent sharps peak intensity. SA-3 has the distinct pattern from the two HT-group, showing single sharp peak which followed with three separated peaks, indicating a better crystallinity from the others SA-PCM.

The operation activity of PCM for TES system highly reliant on the temperature limit of the material before experiencing thermal degradation. It is also important to set the working temperature under the limit to prevent from material fatigue [48], which can reduce the effective lifetime of the PCM. Therefore, obtaining the decomposition profile through TGA evaluation is taken to understand the working limit for the PCM. Figure 3 presents all profiles for tested PCM, showing identic pattern on the degradation behavior which occurs as continuous process. The variation is seen between LT and HT group at the first decomposition. LT-group decomposes generally around 210 °C with varies about 12 °C between each PCM within the same group. For HT-group, decomposition occurs at relatively higher temperature, particularly for SA-1 and SA-2 which happens at 254 °C, while SA-3 degrades above 229 °C. In addition, the decomposition range for HT-group generally longer than LT-group due to higher mass density.

DSC evaluation shows the melting-freezing characteristic as heating-cooling cycle, revealing the physical changes of the PCM (Figure 4). The

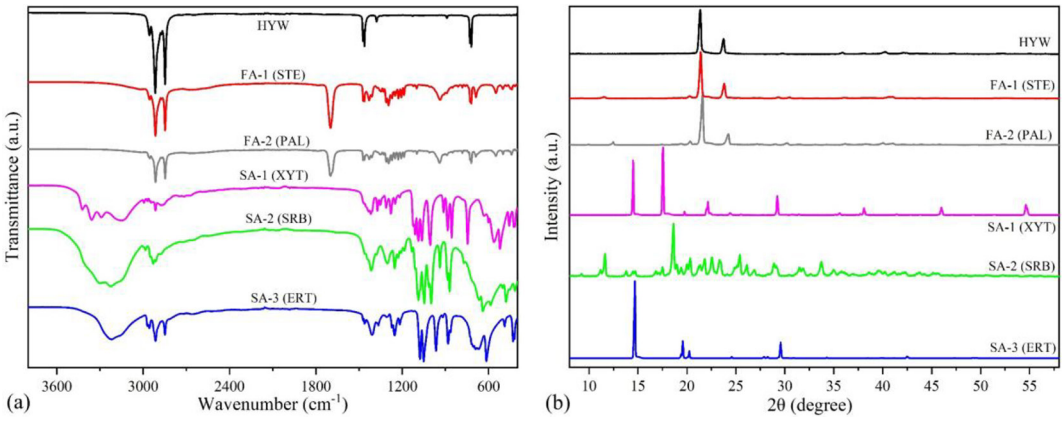

Figure 2. FTIR pattern (a) and crystal characteristic from XRD (b)

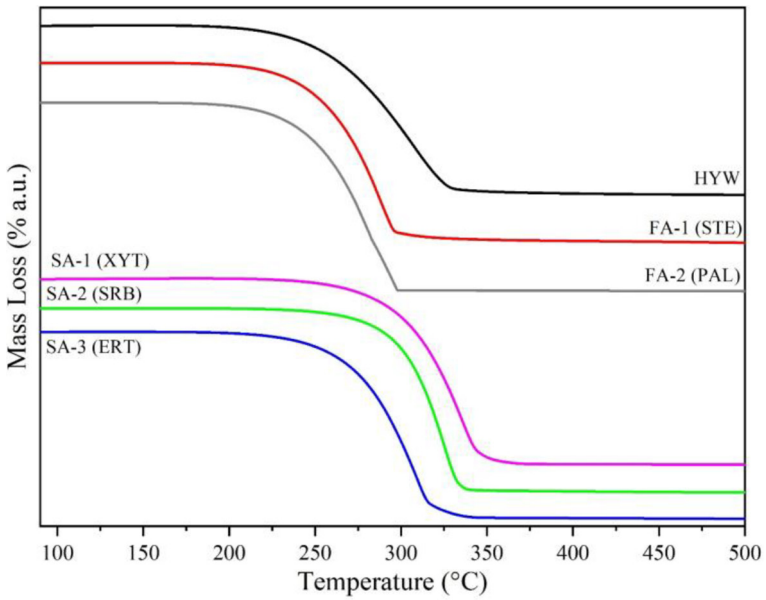

Figure 3. Decomposition temperature from TGA characterization

summary of temperature transition and enthalpy are tabulated in Table 1. The difference in melting range between LT and HT are used as the basis for justifying the category of working temperature for the PCM. LT-group has melting range of 61–64.8 °C. The melting behavior for HYW demonstrate an initial appearance of short curve at peak 44.2 °C before fully melted with peak 61 °C. The pattern for FA-1 and FA-2 are relatively similar with the display of one peak throughout melting stage. The peak melting for the FA-1 and FA-2 varies about 3.5 °C. For the HT-group, SA-1 and SA-2 demonstrates small melting peak deviation, though the cumulative ΔH varies greatly (215.9 J/g for SA-1 and 174.3 J/g for SA-2). SA-3 has the highest melting peak among SA group, coming with temperature 119.4 °C followed with ΔH about 275.6 J/g. The variation on the melting properties become as critical parameter to understand the heating intake performance when operating as TES.

The PCM requires for reversible capability as it affects the releasement of stored energy from heating cycle. The pattern from DSC cooling stage (Figure 4b) shows a recognizable variation between LT and HT group. Particularly, PCM comes from LT group able to show the cooling peak ranging from 53.3 °C to 60 °C. Still, the deviation between melting/freezing peak appeared, indicating the inability of the PCM to achieve ideal transition and associate with supercooling state since the PCM remain in liquid phase below its transition temperature [49]. It makes the PCM incapable to release the latent heat effectively and may bring significant deterioration on the performance of the working TES unit. The utmost condition is found for all HT groups. No freezing peak observed down to 30 °C for two PCM from HT groups (SA-1 and SA-2) which also can be seen from the photograph after the PCMs cooled to room temperature (Figure 4c). Based on literature [50], the releasement of latent heat for the SA-1 and SA-2 require additional trigger to initiate solidification, making it becomes challenging despite their excellent thermal properties. In case of SA-3, indication of the peak is shown at the temperature far below its melting transition. According to [51], factor which correspond to the phenomenon is strong molecular bonding in liquid state, making high energy is required to break the bonding and initiate crystallization close to its melting temperature.

The temperature evolution for each PCM varies notably as the dynamic heating were taken, showing the intercorrelation factor between type of PCM and heating rate. For the STC operation (Figure 5a), solid-liquid transition of FA-1 appears notably between 55.7 to 75.6 °C, which fall within the range of temperature set from DSC evaluation (Table 1). However, the observation for transition of HYW and FA-2 are relatively difficult due to their short charging cycle to achieve the upper temperature charge. It indicates the HYW and FA-2 experience steady melting process, allowing the effective heat input from the source.

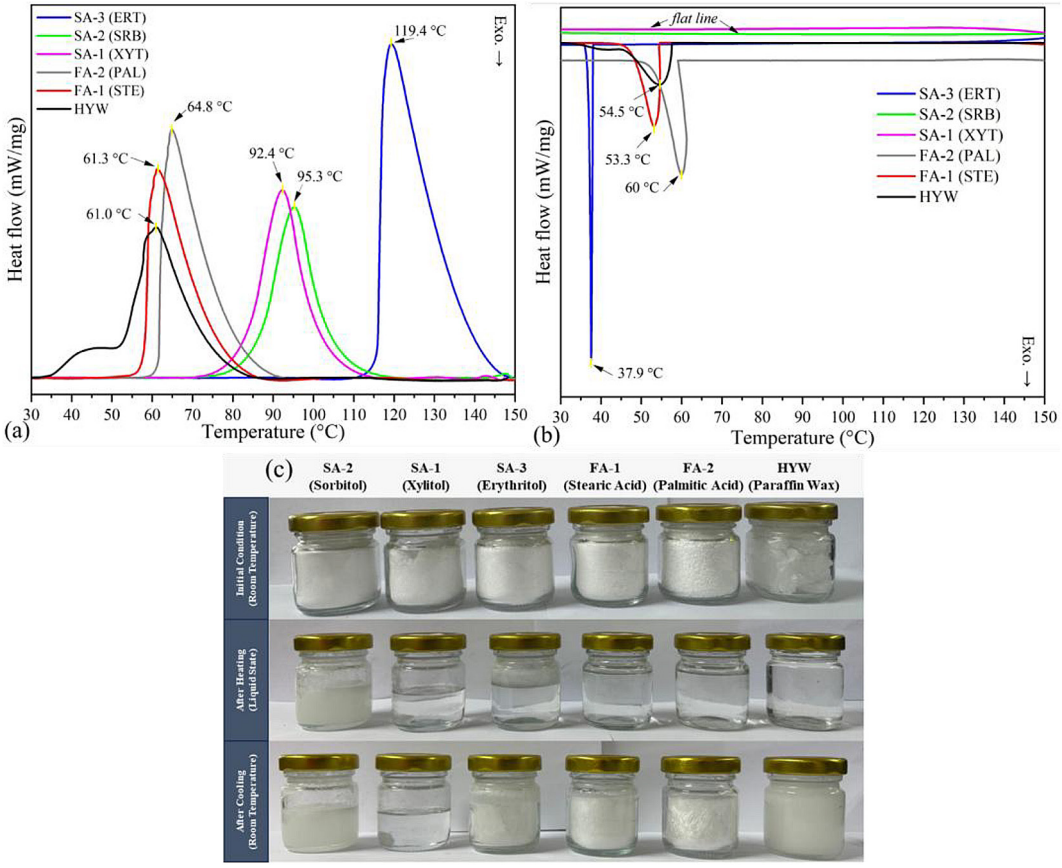

Figure 4. DSC curve (heating (a) and cooling (b) for each PCM and photograph of the PCM after heating-cooling (c)

Table 1. Summary of temperature range and enthalpy from DSC

Group	PCM	Temperature (°C)						ΔH[a] (J/g)
		Heating			Cooling			
		Onset	Peak	End	Onset	Peak	End	
LT	HYW	52.8	61.0	76.4	58.2	54.5	45.9	148.2 (± 4.736)
	FA-1 (STE)	55.5	61.3	84.6	55.1	53.3	43.7	157.8 (± 4.467)
	FA-2 (PAL)	57.3	64.8	91.1	61.4	60.0	48.5	178.5 (± 5.185)
HT	SA-1 (XYT)	71.9	92.4	113.6	-	-	-	215.9 (± 5.853)
	SA-2 (SRB)	76.1	95.3	117.8	-	-	-	174.3 (± 5.093)
	SA-3 (ERT)	108.7	119.4	149.6	38.3	37.9	35.8	275.6 (± 7.924)

Note: [a] the enthalpy (ΔH) calculated from heating (endothermic) cycle.

For HT-group, SA-1 shows a slow temperature increase at 90.3 °C while SA-2 occurs earlier around 75.6 °C, showing the initiation of melting stage for the materials. Increasing the heating power (MTC, Figure 5b) causes two melting step which observed clearly for SA-3 around 50 °C and 102 °C, while the others PCM indicate direct temperature evolution with minimum appearance of transitional region due to higher heating rate from the source.

Rapid charging (Figure 5c) forces the material to absorb the supplied energy quickly. As result, the temperature evolution mostly appears like slope. Despite that, the melting process remain occurs for the material which is shown by several temperature disturbance, indicating the change in heat input to the material due to latent heat takes in place transforming the material from solid to liquid. Specific condition is shown for SA-3 since it able to indicate the transition pattern above

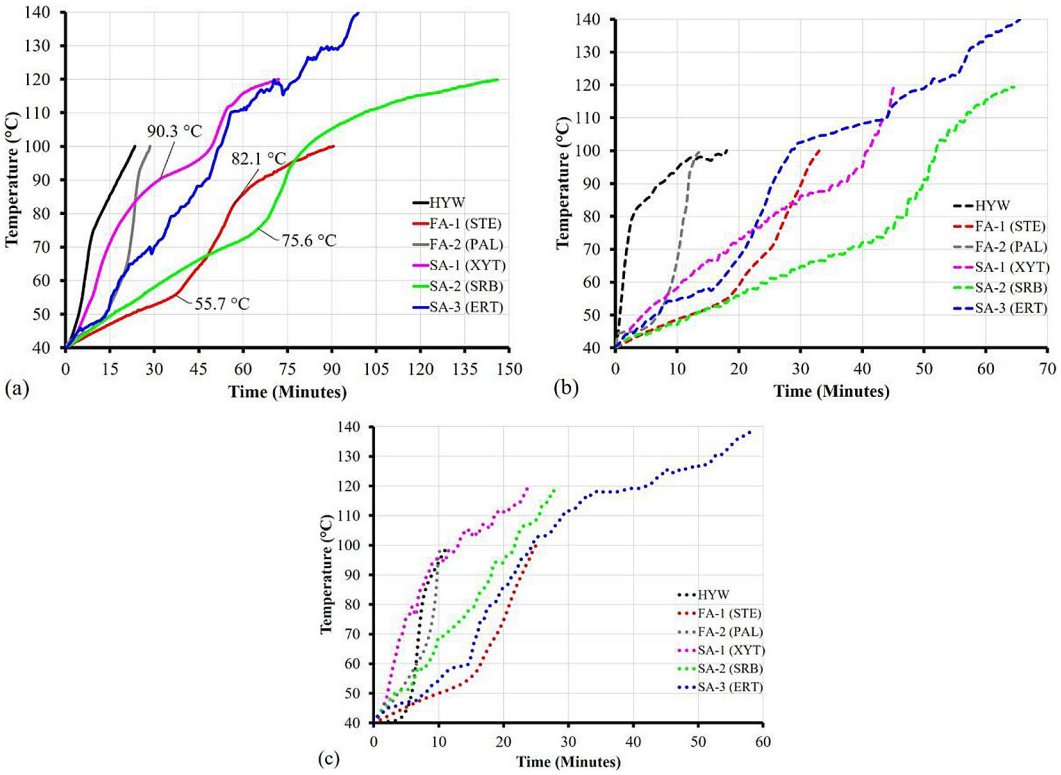

Figure 5. Dynamic thermal charging for the PCMs using STC (a), MTC (b) and RTC (c) operation

110 °C despite the operation under rapid charging cycle. It correlates with the high latent heat and transition temperature of SA-3 (Table 1). The dynamic heating reveals each PCM changes notably on the temperature evolution pattern, demonstrating the complex operational protocol of TES unit which also affected by the low conductivity for typical organic PCM. It forces to support additional modification from the material to enhance its properties [52], including modification within the tank to ensure uniform and steady temperature evolution during charge cycle. Also, the assessment reveals the importance to choose suitable PCM based on the designed heating operation from the TES unit to maintain the effective energy intake.

Releasing the stored heat under different cooling process clearly impact the temperature behavior of the PCM (Figure 6). The LT-group PCM indicates the transition zone (blue arrow, Figure 6a) at temperature 61.6 °C (FA-2), 56.7 °C (FA-1) and 52.3 °C (HYW). The all temperature falls with the liquid-solid transition zone according to the cooling curve from DSC (Figure 4b). The temperature curve for SA-1 and SA-2 drops directly without indicating any disturbance or retardment, clearly implying poor solidification characteristic of the materials which become challenging for the actual TES operation. SA-3 (ERT) demonstrates fluctuate temperature between 100.1–110.3 °C (yellow circle Figure 6a). The pattern shows the initiation of delayed solidification which only starts after the temperature fall to 100.1 °C, resulting in latent heat release and cause brief temperature to increment as observed. Increasing the discharge load using force air (MTD) causes the variation of transition behavior for SA-3 (black arrow Figure 6b) which occurred at 110 °C. For the all LT-group, the zone of solidification initiation remain appears despite some changes occurred due to higher discharge load from the system.

Releasing the heat quickly through RTD scenario affects notably on the shift of transitional phase change temperature. Specifically, the shift appears for FA-1 at 56.5 °C, FA-2 at 60.9 °C and HYW at 47.6 °C (blue arrow Figure 6c). It becomes one crucial indication that dynamic cooling potentially differs the operational of TES unit, which makes operational protocol and control must be set based on the type of PCM and overall system workflow. Moreover, it emphasizes the assessment of TES material cannot be depend solely on DSC curve since large material content may result in different heat distribution as found in actual TES unit. For SA-3, minor

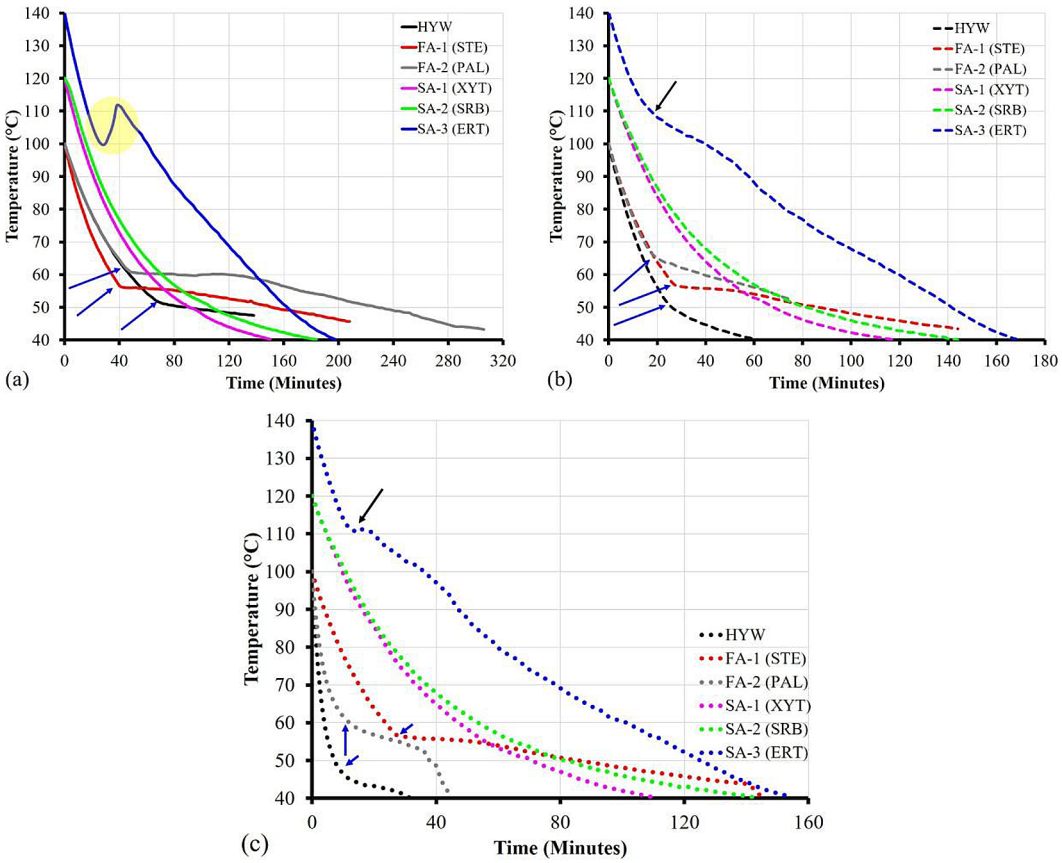

Figure 6. Dynamic thermal discharge for the PCMs using STD (a), MTD (b) and RTD (c) operation

fluctuation is shown at relatively similar temperature around 110 °C (black arrow Figure 6c) and confirms the change in temperature decrement due to phase change of the material. Despite the discharge test were set under different mode, SA-1 and SA-2 remain unable to indicate any sign of solidification and consistently demonstrate direct temperature drop. It makes additional adjustment for the two materials are mandatory to ensure the releasement of latent heat upon cooling cycle.

Specific comparison for the operation activity and type PCM are indicated according to the rating input/output. Despite the test using specific electric power, the variation of thermal properties from the PCM and melting behavior alters the temperature increment rate. Thus, the heating rate is obtained by dividing the total temperature gradient with total duration from the charge cycle [53]. Poor melting behavior for FA-1 causes low increment of rating input with maximum increase from MTC to RTC only 1.36 °C/min (Figure 7a). Significant improvement for FA-2 is found after operating with MDC, which increases about 3.55 °C/min, while HYW indicates a better performance improvement between MTC-RTC. Higher latent heat makes the rating intake becomes lower under the same rating operation. It makes the HT-group generally has lower operation input than LT-group. In addition, SA-1 and SA-2 only increase notably once the operation runs under RTC mode. It directly relates with a better heat distribution under the operation, followed with lower latent heat for the materials. The overall rating for SA-3 is much lower than all tested PCM, proving the impact of high melting point and latent heat that affect the rating input. Lower rating input potentially increases the heat losses during charge, making essential adjustment like insulation [54] or modification are important as prevention.

Heat release stage becomes the essential function on the activity of TES unit (Figure 7b). The interesting result is shown for HYW and FA-2 as it able to indicate consistent outcome, demonstrating steady rating increment as the discharge taken using higher load. However, FA-1 shows the lowest value due to poor discharge behavior which correlate with its freezing mechanism. The HT-group generally shows a consistent performance than LT-group. It allows for additional benefit, especially for adjusting operation activity

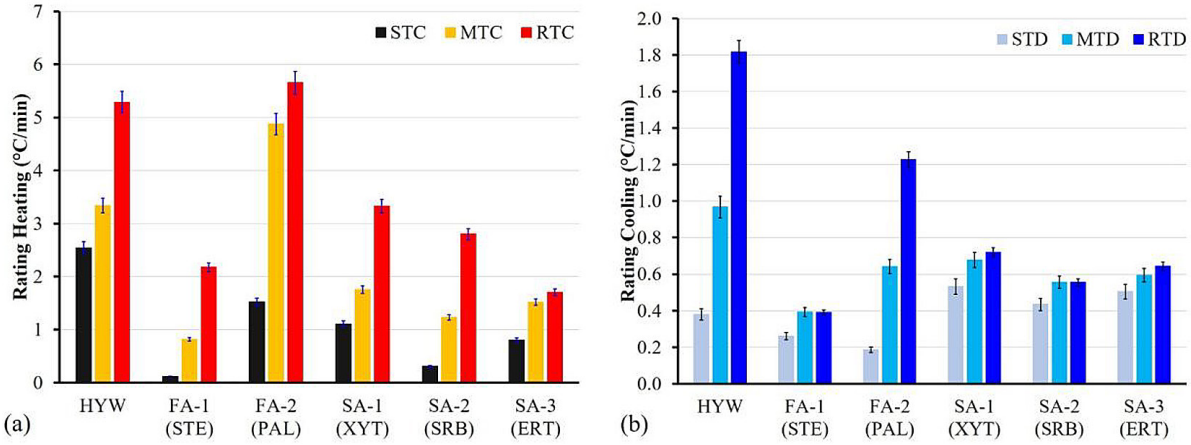

Figure 7. Rating comparison between LT-HT group for heating (a) and cooling (b)

when using HT-group for dynamic rating energy transfer. Despite that, deeper consideration is required for SA-1 and SA-2 for exploring necessary modification to initiate latent heat release from discharge process. It potentially brings additional benefit for using SA-1 and SA-2 as suitable PCM for TES system.

CONCLUSIONS

The evaluation from various PCM is performed as specific approach to address the complex interrelation between the properties of PCM and dynamic operation of TES unit. The three-step mode heating-cooling as a function energy intake-release shows a clear distinction on the behavior change of each PCM. For the LT group, a stable and consistent pattern are achieved as the intake heating increased for HYW and FA-2 (PAL). One specific concern is shown for FA-1 (STE) which indicated insignificant changes despite the heating intake is increased. In case of HT-group, SA-1 (XYT) and SA-2 (SRB) indicates a reliable improvement under the variation heating mode while high ΔH and transition temperature for SA-3 (ERT) causes minimal impact on the change of heating rate, showing the lowest value compared to others PCM from HT-group. The dynamic cooling principally indicates HYW and FA-2 (PAL) with relevant improvement on the rate while the FA-1 (STE) still remarkably unchanged. Also, HT-group consistently shows the lowest cooling rate from the three scenarios, showing the impact of supercooling condition, particularly for SA-1 and SA-2. The ideal pattern improvement technically achieved by SA-3 (ERT) which shows the value increases slightly for each different cooling load. The finding from this work implies further modification for the operation of TES unit to accommodate the dynamic behavior for each PCM. It is recommended to consider the given factor for designing TES unit, including the enhancement of storage tank to maximize heat transfer and dynamic rating input to adjust the temperature changes for charge cycle. Also, modification for the material, particularly for SA-1 and SA-2 are highly recommended for future exploration, such as adding nucleating agent, combination with SA that able to recrystalize, and mechanical stirrer. The overall factor are expected to improve the operation of TES unit and deliver a better performance for thermal system.

Acknowledgement

The authors acknowledge the support of the Ministry of Higher Education, Science, and Technology of the Republic of Indonesia through the 2026 Fundamental Research Grant Scheme.

REFERENCES

1. Ismail I, Mulyanto AT, Rahman RA. Development of free water knock-out tank by using internal heat exchanger for heavy crude oil. EUREKA, Physics and Engineering 2022; 77–85.
2. Wiyono A, Aziz M, Sholehudin A, et al. Syngas optimization and tar reduction via multistage catalytic gasification: Effects of catalyst pore, catalyzer stage, and temperature profile. South African Journal of

Chemical Engineering 2024; 48: 246–253.

3. Ismail, John J, Pane EA, et al. Experimental evaluation for the feasibility of test chamber in the open-loop wind tunnel. WSEAS Transactions on Fluid Mechanics 2021; 16: 120–126.
4. Ben Smida M, Sakly A. A novel crow search algorithm-based maximum power point tracking method for wind energy conversion systems. Advances in Science and Technology Research Journal 2025; 19: 189–202.
5. Ismail, Rahman RA, Haryanto G, et al. The optimal pitch distance for maximizing the power ratio for savonius turbine on inline configuration. International Journal of Renewable Energy Research 2021; 11: 595–599.
6. Wiyono A, Mohd Zulkifli NW, Wan Daud WMA, et al. Review on synthesis methods of carbon nanotubes as activated carbon composites based on biomass for supercapacitors in electric vehicles. Energy Technology 2025; 13.
7. Algailani HM, Al-Nassar SI, Mahmoud AK, et al. Synthesis of bio-nanocomposite coating (silver-multi wall carbon nano tubes) by electroless plating method. Materials Today: Proceedings 2023; 2–6.
8. Kumar A, Kumar R. Enhancement and estimation of thermo-physical properties of organic-phase change materials (O-PCMs) and their applications in solar thermal technologies: A review. Journal of Energy Storage 2024; 101: 113741.
9. Roux D Le, Serra S, Sochard S, et al. Sensibility analysis and environmental impact of a system combining a solar-assisted heat pump and PCM storages. Energy Conversion and Management 2024; 322.
10. Le Roux D, Serra S, Sochard S, et al. Dynamic simulation of a combined solar system including phase change material storage and its experimental validation. Renewable Energy 2024; 234: 121112.
11. Le Roux D, Noël H, Fuentes A, et al. Review on horizontal underground thermal energy storage (HUTES). Journal of Energy Storage 2026; 147.
12. Vengadesan E, Muralidharan S, Vishnu SK, et al. Enhanced conductivity and shape-stable paraffin wax phase change material incorporating banana stem biochar. Journal of Energy Storage 2026; 154.
13. Theriselvam K, Arumugaprabu V, Uthayakumar M. Experimental study on the effect of biochar loaded with paraffin wax that acts as a phase change material and epoxy-coated shape-stabilized PCM composite on leakage resistance and shape stability. Materials Today Communications 2026; 52: 115156.
14. Alturki TMM, Karaağaç MO, Ergün A. Performance analysis of a stationary parabolic trough solar collector with a flat metallic receiver incorporating paraffin wax PCM. Energy Conversion and Management 2026; 356.
15. C N D, Behura AK. Thermophysical characterization and reliability analysis of binary composite nano doping on stearic acid-acetamide eutectic PCM. Materials Today Sustainability 2024; 26: 100804.
16. Hammami N, Patry S, Geneste A, et al. Stearic acid fatty esters as biobased phase change materials for building applications: Structure–property relationships and climate-specific suitability. Journal of Energy Storage 2026; 153: 120869.
17. Dubey A, Dubey A, Arora A. Machine learning based prognostic analysis of a hybrid solar still coupled with evacuated tube collector and stearic acid: A comprehensive 4-E assessment. Solar Energy Materials and Solar Cells 2026; 298: 114165.
18. El Majd A, Arkame Y, Sair S, et al. Shape-stabilized capric-palmitic acid/g-C3N4 composite phase change material for efficient Photothermal conversion and low-temperature heat storage. Journal of Energy Storage 2025; 133: 118107.
19. Ranjane PR, Pv G, Kulkarni PS. Polyurethane composites with covalently immobilized polyethylene glycol-palmitic acid as thermal energy storage material. Thermochimica Acta 2026; 759.
20. Liu H, Deng Y, Wu F, et al. Flexible, recyclable and biodegradable polyvinyl alcohol/cellulose nanofibers/palmitic acid phase change composites toward sustainable thermal management. Chemical Engineering Journal 2026; 528: 172360.
21. Jarimi H, Su Y, Riffat S. Assessing the potential of binary and ternary supercooled sugar alcohol-based PCMs as a thermal battery. Applied Thermal Engineering 2026; 292: 130268.
22. El Hadi Attia M, Sathyamurthy R, Arunkumar T, et al. Bio-based sustainable organic eutectic PCMs for thermal energy systems: Comprehensive assessment. Renewable and Sustainable Energy Reviews 2026; 226: 116397.
23. Yadav VK, Ghosh P, Sarkar J. Experimentation and optimization of a novel PCM-based thermal storage-cum-exchanger using steel wire mesh. Applied Thermal Engineering 2026; 290: 130100.
24. Wu YF, Zhang RL, Li ZY, et al. Development and screening of xylitol-based binary eutectic phase change materials with high latent heat of fusion for the temperature range of 70–90 °C. Journal of Energy Storage 2025; 129: 117328.
25. Navarro M, Gracia Z, Asín J, et al. Rheological study on xylitol crystallization for its use as phase change material: analytical and statistical analysis. Solar Energy Materials and Solar Cells 2025; 292.
26. Chenxu Y, Shao X, Wang B, et al. Bubbling triggered crystallization of xylitol phase change material for controllable heat retrieval: The subcooling effect. Solar Energy Materials and Solar Cells 2024; 268: 112744.

27. Hou X, Xing Y, Xu Z, et al. Design and experimental analysis of a cooling system with erythritol/xylitol PCM thermal energy storage. Journal of Energy Storage 2024; 87.
28. Fang Y, Shi Q, Huang X, et al. Erythritol-based phase change materials: Supercooling enhancement and adaptive heat-triggered release for extreme environmental thermal applications. Journal of Energy Storage 2025; 140: 118982.
29. Wusiman K, Wang T, Shi L, et al. A novel evaluation method for thermal stability of erythritol as phase change materials. Thermal Science and Engineering Progress 2025; 59: 103303.
30. Liu X, Wu F, Lv L, et al. Performance of solid particles as thermal storage media in thermal power flexibility retrofits: Effects of charging and discharging flow rates on single piece stacking bed. Energy 2024; 308: 132950.
31. Yuan P, Cui Y, Li H, et al. Thermal response analysis of sand-based thermal storage floors for rural heating under dynamic conditions: Effects of key structural and heating parameters. Journal of Energy Storage 2026; 169: 122818.
32. Ahmadihosseini A, Tavanaei Sereshgi F, Hassani F, et al. Thermophysical behavior of basalt and serpentinite under variable temperature and heating rate for rock thermal energy storage application. Journal of Energy Storage 2026; 158: 121815.
33. Dawood F, Al-Bawee A, Alrubaiy AAAG. Microstructural and thermal property modifications of Sn-43Bi solder alloys via selective alloying with Se, In, Zn, and Al. Advances in Science and Technology Research Journal 2025; 19: 273–284.
34. Jiang R, Xia M, Du Y, et al. Investigations on charging-discharging performance and heat capacity management of latent thermal energy storage-based thermal batteries. Energy and Buildings 2026; 365: 117683.
35. Shahsavar A, Shahmohammadi M, Jafari M, et al. Exploring ultrasonic-assisted phase change material for thermal management in battery systems under variable discharge rates. International Communications in Heat and Mass Transfer 2026; 175: 111094.
36. Baghaei Oskouei S, Bayer Ö. Performance improvement in a vertical latent thermal energy storage tank with crossing heat transfer tubes. Journal of Energy Storage 2024; 88.
37. Wu Z, Niu J, Liu Z, et al. NiCo@EG-based composite PCMs with boosted thermal conductivity and photothermal conversion efficiency for solar energy harvesting. Solar Energy Materials and Solar Cells 2024; 278.
38. Dai R, Wei M, Zheng S, et al. Experimental investigation on thermodynamic performance of a copper foam-based cascaded latent heat storage tubes. Applied Thermal Engineering 2024; 248: 123312.
39. Pardillos-Pobo D, González-Gómez PA, Laporte-Azcué M, et al. Thermo-economic design of an electric heater to store renewable curtailment in solar power tower plants. Energy Conversion and Management 2023; 297.
40. Rahman RA, Sulistyo, Utomo MSKTS, et al. Experimental evaluation on the power characteristic of direct-photovoltaic charging for thermal storage equipment. Mechanical Engineering for Society and Industry 2024; 4: 115–122.
41. Liang Y, Wang D, Li Y, et al. Novel approach to remote rural heating: Direct coupled photovoltaic electric heater underfloor heating system with phase change materials. Applied Thermal Engineering 2024; 250: 123525.
42. Alshuraiaan B. Efficient utilization of PCM in building envelope in a hot environment condition. International Journal of Thermofluids 2022; 16: 100205.
43. Rahman RA, Sulistyo, Utomo MSKTS, et al. Performance evaluation of enhanced clustered latent heat system for air heater using modified organic material. International Journal of Thermofluids 2024; 23: 100807.
44. Surya A, Prakash R, Nallusamy N. Heat transfer enhancement and performance study on latent heat thermal energy storage system using different configurations of spherical PCM balls. Journal of Energy Storage 2023; 72: 108643.
45. Firman LOM, Rahmalina D, Ismail, Rahman RA. Hybrid energy-temperature method (HETM): A low-cost apparatus and reliable method for estimating the thermal capacity of solid-liquid phase change material for heat storage system. HardwareX 2023; 16: e00496.
46. Rahmalina D, Rahman RA, Ismail. Increasing the rating performance of paraffin up to 5000 cycles for active latent heat storage by adding high-density polyethylene to form shape-stabilized phase change material. Journal of Energy Storage 2022; 46: 103762.
47. Rahman RA, Sulistyo, Suryo Utomo MSKT, et al. The optional approach in recycling plastic waste for energy storage application: A detailed evaluation of stabilized–hexadecanoic acid/plastic. Case Studies in Chemical and Environmental Engineering 2024; 9: 1–5.
48. Mohamed MT, Helal RA, Nawi SA, et al. Identifying regularities of high temperature on constant and variable fatigue life of aa7075-al2o3 nanocomposite fabricated by stir casting method. Eastern-European Journal of Enterprise Technologies 2023; 2: 35–41.
49. Shamseddine I, Pennec F, Biwole P, et al. Supercooling of phase change materials: A review. Renewable and Sustainable Energy Reviews 2022;

158: 112172.

50. Lv L, Huang S, Cen K, et al. Experimental study of screening polyols and their binary eutectic phase change materials for long-term thermal energy storage. Journal of Cleaner Production 2023; 399: 136636.
51. Liu H, Jing J, Liu J, et al. Sugar alcohol-based phase change materials for thermal energy storage: Optimization design and applications. Renewable and Sustainable Energy Reviews 2024; 199: 114528.
52. Al-Bawee A, et al. Effect of alumina nanoparticles on the microstructure, mechanical, and thermal properties of penta bismuth-tin-based solder alloys. AIMS Materials Science 2026; 13: 63–79.
53. Syahbana MSL, Kurniawan Y, Ismail I. Experimental study on the effect of different HTF discharges to increase efficiency of a latent heat storage system using a spiral coil heat exchanger with different fins. International Journal of Thermophysics 2024; 45: 1–17.
54. Mahan HM, Katawy A, Shabeeb OA, et al. Analyzing thermal insulation of concrete polymer by adding mineral wool. Advances in Science and Technology Research Journal 2025; 19: 430–439.